INFECTION AND IMMUNITY, Nov. 2002, p. 6346–6354 Vol. 70, No. 11
0019-9567/02/$04.00+0 DOI: 10.1128/IAI.70.11.6346–6354.2002

Transcriptional Analysis of *Rickettsia prowazekii* Invasion Gene Homolog (*invA*) during Host Cell Infection

Jariyanart Gaywee,[1] Suzana Radulovic,[1] James A. Higgins,[2] and Abdu F. Azad[1]*

Department of Microbiology and Immunology, University of Maryland School of Medicine, Baltimore, Maryland 21201,[1] and USDA Agricultural Research Service, Beltsville, Maryland 20705[2]

Received 14 May 2002/Returned for modification 12 July 2002/Accepted 8 August 2002

An invasion gene homolog, *invA*, of *Rickettsia prowazekii* has recently been identified to encode a member of the Nudix hydrolase subfamily which acts specifically on dinucleoside oligophosphates (Np_nN; $n \geq 5$), a group of cellular signaling molecules known as alarmones. InvA is thought to enhance intracellular survival by regulating stress-induced toxic nucleotide levels during rickettsial infection. To further characterize the physiological function of InvA, the gene expression pattern during various stages of rickettsial intracellular growth was investigated. Using semiquantitative reverse transcription-PCR (RT-PCR) and real-time fluorescent probe-based quantitative RT-PCR, a differential expression profile of *invA* during rickettsial host cell infection was examined. The *invA* transcript temporarily increased during the early period of infection. Expression of rickettsial *groEL*, a molecular indicator of cellular stresses, was also shown to be upregulated during the early period of infection. Furthermore, *invA* was cotranscribed in a polycistronic message with *rrp*, a gene encoding the response regulator protein homolog, which is a part of a two-component signal transduction system. These results support our earlier findings that under such stress conditions dinucleoside oligophosphate pyrophosphatase may function as a buffer, enhancing rickettsial survival within the cytoplasm of a eukaryotic cell. The expression of rickettsial dinucleoside oligophosphate pyrophosphatase may be regulated by a part of the two-component signal transduction system similar to that described for response regulators in other bacterial systems.

Rickettsia prowazekii, the causative agent of epidemic typhus, is a gram-negative, obligate, intracellular bacterium that is able to grow within the cytoplasm of eukaryotic host cells (12). In addition to sporadic cases occurring in the foci of endemicity, epidemic typhus, a disease considered to be of historical importance, still remains capable of producing severe morbidity and mortality in displaced populations where poverty, war, and poor vector control exist (4). A recent outbreak of epidemic typhus in refugee camps in Burundi, involving over 30,000 human cases, testifies to the continued threat that *R. prowazekii* poses to human health (21). Classically, *R. prowazekii* is maintained in a cycle involving human and body lice, *Pediculus humanus*, and the organism is transmitted to humans by direct contact with contaminated body louse feces (5). Infection of human body lice involves the epithelial lining of the midgut (5). Within the mammalian host, rickettsiae invade the endothelial cells preferentially, although the other cell types, such as epithelial cells and macrophages, are also affected (12).

Rickettsial entry into eukaryotic cells occurs via induced phagocytosis, a rapid escape from the phagosome into the host cytoplasm, followed by massive replication and host cell death to facilitate rickettsial release (12). Although the biological bases underlying rickettsial entry, intracellular growth, and host cell lysis have been studied in detail, delineating the molecular mechanisms involved in this unique, intracytoplasmic parasitism remains an important subject of research.

New opportunities arising from the completion of the *R. prowazekii* and *Rickettsia conorii* genomes now enable us to select rickettsial genes for characterization studies, based on their homology to genes with a known function in closely related bacteria (3, 18). Among these was *invA*, a 486-bp gene that showed homology to host cell invasion genes of other bacterial pathogens (3, 6, 10, 17, 18). We have recently cloned and characterized *R. prowazekii invA* as encoding a member of the subfamily of the Nudix hydrolases, a group of diverse enzymes that catalyze the hydrolysis of nucleoside diphosphate derivatives (10). Based on the observation that InvA hydrolyzes dinucleoside oligophosphates, yielding ATP as one of the reaction products, it has been proposed that this invasion protein likely plays a role in enhancing intracellular survival of the bacteria (10). By regulating the levels of toxic dinucleoside oligophosphates that accumulate during the oxidative stress following bacterial invasion by converting these compounds into a useful molecule such as ATP, rickettsiae have developed a successful mechanism for intracytoplasmic living (10). Aside from the enzymatic activity, other aspects of the biological function of InvA remain to be defined. Previous studies of *ygdP*, the *invA* homolog in *Escherichia coli* K1, have shown that bacterial invasiveness and the transcription of *ygdP* significantly increased under in vitro growth conditions mimicking a serum environment, compared with that under normal growth conditions (6, 7). These data indicate that the expression of *ygdP* is environmentally regulated and is associated with bacterial invasive capability (6, 7). Investigation of *R. prowazekii invA* transcription during the invasion process may provide information as to how a dinucleoside oligophosphate pyrophosphatase might facilitate rickettsial internalization in host cells. In this communication, the transcriptional pattern of *invA* in *R. prowazekii*-infected cell culture is described. In ad-

* Corresponding author. Mailing address: Department of Microbiology and Immunology, University of Maryland School of Medicine, 655 West Baltimore St., Baltimore, MD 21201. Phone: (410) 706-1341. Fax: (410) 706-0282. E-mail: aazad@umaryland.edu.

dition, the expression profiles of the genes encoding a response regulator protein homolog, Rrp, and the heat shock protein, GroEL, are discussed.

MATERIALS AND METHODS

Preparation of *R. prowazekii*-infected Vero cells. A confluent monolayer of African green monkey kidney cells (Vero cell; ATCC C1008) in Eagle's minimum essential medium supplemented with 5% fetal calf serum and 2 mM L-glutamine was inoculated with *R. prowazekii* (Madrid E) at a multiplicity of infection of 80 rickettsiae per cell, as previously described (20). After absorption of rickettsiae to the host cells for 30 min at room temperature, freshly prepared culture medium was added and the cultures were shifted to 37°C for 30 min to allow rickettsial entry and subsequently incubated at 34°C in a humidified atmosphere with 5% CO_2. To determine the transcriptional kinetics of *invA* during rickettsial infection, samples representing various stages of the rickettsial life cycle (Fig. 1A), including attachment (time zero, before temperature shift), internalization (10 min, 30 min after temperature shift), early intracytoplasmic living (1, 2, and 4 h after temperature shift), replication (8 h, 12 h, 24 h, and 2 days after temperature shift), and exit by cell lysis (8 days postinfection) were collected. With the exception of the preinfection samples (time zero), infected cells were harvested at each time point, washed in phosphate-buffered saline to remove extracellular bacteria, and pelleted at 5,000 × *g* for 10 min. A preinfection (time zero) sample representing attached rickettsiae to the host cells was harvested by scraping the cultured cells, followed by centrifugation at 10,000 × *g* for 30 min. The cell pellet for each time point was immediately aliquoted, rapidly frozen, and stored at −80°C until use.

RNA extraction. Total RNA was isolated from an aliquot of frozen *R. prowazekii*-infected Vero cells by using the RNAqueous-Midi kit (Ambion, Austin, Tex.) according to the manufacturer's protocol. Negative control RNA from uninfected Vero cells was extracted in parallel procedures. RNA samples were then treated with RNase-free DNase (Stratagene, La Jolla, Calif.) at 37°C for 30 min, followed by heat inactivation at 70°C for 5 min. To verify the efficiency of genomic DNA decontamination, 45-cycle PCR of host cell β-actin and rickettsial 16S rRNA genes was performed on DNase-treated RNA, omitting a reverse transcription (RT) step. The concentration and quality of isolated RNA was examined by spectrophotometer and formaldehyde agarose gel electrophoresis. Aliquots of the DNase-treated total RNA samples were stored at −80°C until use.

RT. First-strand cDNA was synthesized using an Omniscript reverse transcription kit (Qiagen, Valencia, Calif.) and random hexamers (Stratagene). Each 20-μl reaction mixture contained 2 μg of DNase-treated total RNA, 1× RT buffer, 500 μM concentration of each deoxynucleoside triphosphate (dNTP), 1 μM random hexamers, 10 U of RNase inhibitor (Stratagene), and 4 U of Omniscript reverse transcriptase. RT was carried out at 37°C for 60 min, followed by RT inactivation for 5 min at 95°C. The resulting cDNA samples were stored at −80°C until use.

RT-PCR analysis of gene expression during rickettsial host cell infection. To examine the expression pattern of *invA* during rickettsial host cell infection, a modified version of semiquantitative RT-PCR previously established in our laboratory was utilized (14, 15). The resulting cDNAs at different stages during rickettsial host cell infection were amplified using the specific primers listed in Table 1. The eukaryotic β-actin and the rickettsial 16S rRNA genes were used as the internal controls for RT-PCR. Each PCR was carried out in a total volume of 50 μl containing 1/5 of the RT product (equivalent to 0.4 μg of cDNA) as a template, 1× PCR buffer, 1.5 mM $MgCl_2$, 200 nM concentrations of dNTPs, 0.2 μM concentrations of primers, and 1 U of Platinum *Taq* polymerase (Invitrogen, Carlsbad, Calif.). The optimal amplification efficiency for each gene was previously established by optimization of the magnesium concentration, the annealing temperature, and the cycle number specific for each individual gene. The optimal annealing temperature and the cycle number for each individual gene are shown in Table 1. Amplification was performed with an initial denaturing of 95°C for 5 min followed by 35 or 45 cycles for each individual transcript of 94°C for 15 s, 55, 57, or 62°C for 45 s, 68°C for 50 s, and a final extension step of 68°C for 7 min (Table 1). Twenty microliters of PCR product was electrophoresed on a 1% agarose gel stained with 10 μg of ethidium bromide/ml and examined under a UV transilluminator. To quantitate and compare mRNA levels, the gels were photographed utilizing an Alpha Imager (Alpha Innotech Corporation, San Leandro, Calif.), and the intensity of the bands was analyzed by using the densitometry function. The relative band intensities in each experiment were normalized to the intensity of the internal control bands running in parallel. The ratio of the sample intensity to that of the corresponding internal controls from three experiments was expressed as the mean ± standard error and was plotted against the time points of the analysis. A one-way analysis of variance (ANOVA) was used to determine statistical differences between columns (treatment) and residual (within columns).

Real-time fluorescent probe-based Q-RT-PCR analysis of gene expression. To assess the kinetics of *R. prowazekii invA* expression during the infection cycle, a real-time quantitative RT-PCR (Q-RT-PCR) using TaqMan probe technology (11) was performed on samples representing the different stages during rickettsial host cell interaction. *R. prowazekii* 16S rRNA and eukaryotic β-actin genes were used as endogenous controls to confirm the quality of the template and, in the case of *invA*, to normalize the expression levels between samples. Primers and probes used in this study are listed in Table 2. For two-step real time Q-RT-PCR, 0.4 μg of cDNA was added to a 50-μl reaction mixture containing 1× TaqMan PCR master mix (Applied Biosystems, Foster City, Calif.), 200 nM concentrations of dNTPs, 1.5 mM $MgCl_2$, 200 nM concentrations of each primer, 100 nM fluorescent probe, and 1 U of Platinum *Taq* DNA polymerase (Invitrogen). Thermal cycling conditions for primers and probes were optimized for magnesium concentration and annealing temperature. Amplification and detection was performed on an ABI Prism 7700 sequence detection system (Applied Biosystems). The amplified conditions were 95°C for 3 min and 45 cycles of 94°C for 15 s, 58°C for 45 s, and 72°C for 45 s.

For single-tube RT-PCR assays, the Invitrogen Superscript kit was used according to the manufacturer's instructions. One microliter of RNA (equivalent to 0.20 to 0.35 μg) was added to a 50-μl final reaction volume containing 1 μl of Superscript enzyme, 25 μl of 2× reaction buffer, 1 μl (50 pmol) of each primer, 1 μl (10 pmol) of probe, and 21 μl of water. Cycling conditions were 30 min at 55°C, 2 min at 95°C, and 45 cycles of 15 s at 95°C, 30 s at 58°C, and 45 s at 72°C. The single-step RT-PCRs were conducted on the Stratagene Mx4000 instrument.

Cycle threshold (C_t) values were automatically calculated by the instrument for each reaction. These values were defined as the cycle number at which the fluorescence generated by the released reporter dye molecule exceeds a fixed threshold value above the baseline. Quantification of *invA* and 16S rRNA gene expression was done using the comparative $\Delta\Delta C_t$ method as described elsewhere (User Bulletin no. 2, Applied Biosystems, 1997). Briefly, expression of the *invA* gene for each time point was normalized using the C_t value for the endogenous reference, the 16S rRNA gene. The sample-time point combination with the lowest level of *invA* gene expression was designated a calibrator, with a gene expression level of 1.0, and *invA* expression in the other samples was given as a multiple of this sample. For the two-step RT-PCR assays, the calibrator was designated to be the preinfection sample (time zero), and for the single-tube RT-PCR assays, the 12-h sample was used. Statistical analysis of real-time Q-PCR data was done using the ProStat software package (Poly Software International, Pearl River, N.Y.). Briefly, the mean ± standard deviation C_t data for each time point ($n = 3$ replicates) were compared using a one-way ANOVA with accompanying multiple comparison tests.

RESULTS

To better understand the role of InvA in rickettsial host cell invasion, transcription of *invA* at various stages during in vitro host cell infection was investigated. Monitoring *invA* expression in Vero cells permitted a high degree of control over the time course of infection and resultant sample collection. Semiquantitative RT-PCR was chosen due to its high sensitivity in mRNA quantification, compared to that of Northern hybridization. In this study, it was impractical to obtain rickettsial RNA without host cell RNA contamination. To detect rickettsial message in a high background of host cell mRNA, we optimized RT-PCR conditions to yield the highest sensitivity with the least amount of background. The sensitivities of PCR performed at the optimal cycle parameters were 4 and 100 copies of plasmid DNA (PCR2.1:Rp16SrRNA and PCR2.1:Rp*invA*), or 5 ng and 20 ng of cDNA (mixture of rickettsial and host cell cDNA) for rickettsial 16S rRNA and *invA*, respectively (data not shown).

RT-PCR was performed on synthesized cDNA from samples collecting during specific stages of the rickettsial life cycle in the host cell, including entry, escape from the phagosome,

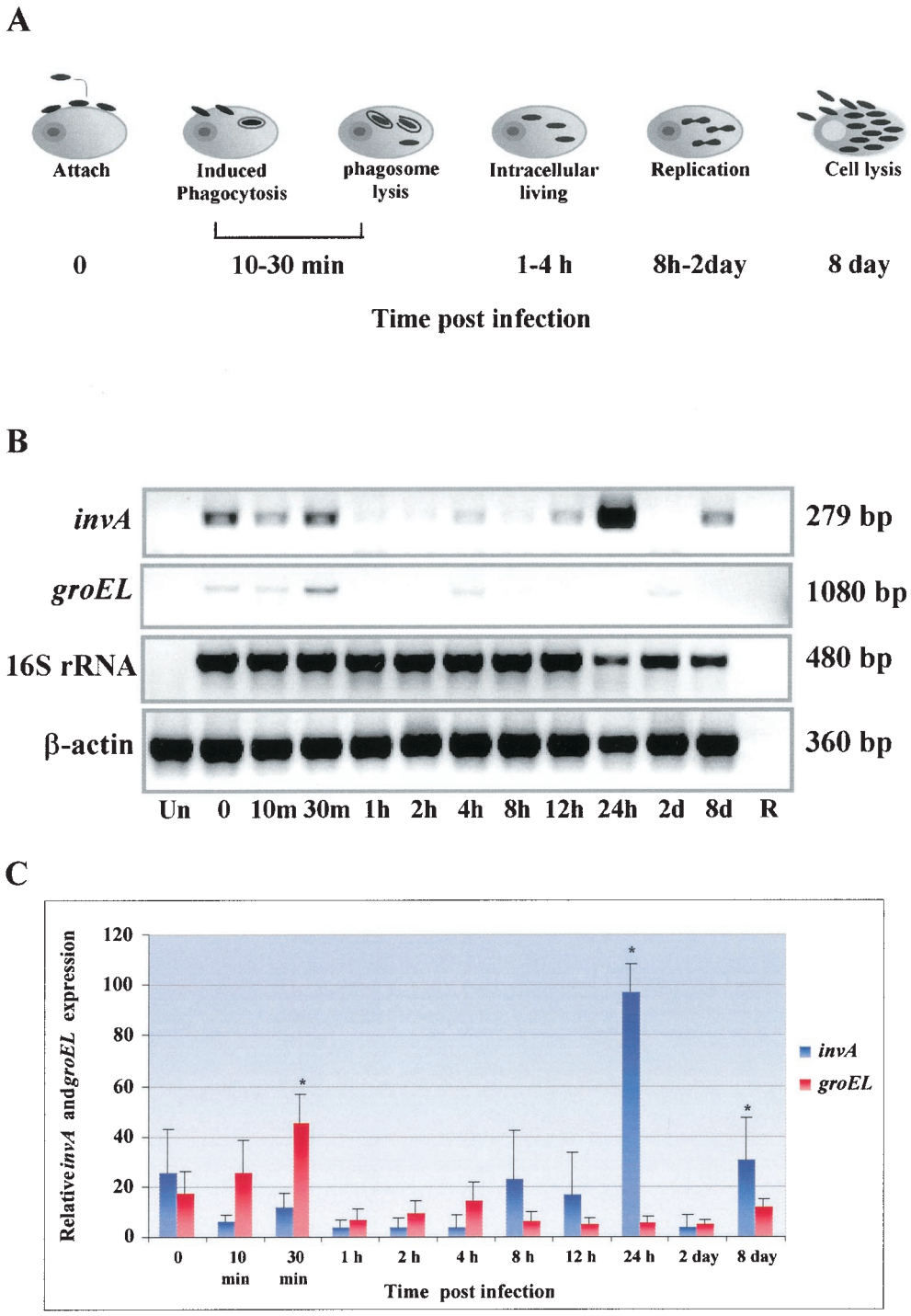

FIG. 1. Kinetics of *invA* and *groEL* transcription during in vitro rickettsial infection. (A) Various stages of the intracellular life cycle of typhus group rickettsiae, such as attachment, internalization, early intracytoplasmic living, replication, and exit by host cell lysis. (B) The transcription of *invA* and *groEL* in *R. prowazekii*-infected Vero cells at various stages of rickettsial infection was determined by semiquantitative RT-PCR. Amplified products were electrophoresed on 1% agarose gels stained with ethidium bromide, shown in negative. The rickettsial 16S rRNA and mammalian β-actin genes were used as endogenous controls to confirm an equivalent quantity of template loading. The size of amplified fragment is indicated on the right. (C) Densitometric analysis of *invA* and *groEL*. The levels of expression were quantitated by using the densitometry function of the Alpha Imager software. The densitometric result of each time point was normalized to the internal control running in parallel. The ratio of sample intensities to their internal controls, expressed as mean ± standard error, was plotted on the *y* axis against time postinfection. A one-way ANOVA was used to determine statistical differences between columns (treatment) and within columns (residual). ∗, significant difference at a P level of <0.05.

TABLE 1. Primers for RT-PCR

Gene (GenBank access. no.)	Sequence	Nucleotide position	PCR product (bp)	Annealing temp. (°C)	Amplified cycles
Vero cell β-actin (AB004047)	Forward primer: 5′-CTGGCACCACACCTTCTACAATG-3 Reverse primer: 5′-AATGTCACGCACGATTTCCCGC-3′	265–287 646–625	382	57	35
R. prowazekii 16S rRNA (M21789)	Forward primer: 5′-TCCACGCCGTAAACGATGAG-3′ Reverse primer: 5′-TGCTTCCCTCTGTAAACACCATTG-3′	770–789 1229–1206	460	62	35
R. prowazekii invA (AJ235271)	Forward primer: 5′ TAGACCAGGGGTAGGCATGATG 3′ Reverse primer: 5′ AACCAGCGTTGTTTTTGTCCAC 3′ Reverse 140: 5′CCACCTTGAGGCATTTGCCATGAAGATATTTTTG3′	12711–12732 12475–12454 12812–12780	279 512[a]	62 55	45 45
R. prowazekii rrp (AJ235271)	Forward primer: 5′-ACGGTCATCAAGCAGGGGATAAGG-3′ Reverse primer: 5′-AACTCTAACTCTTTCCGCAG-3′	12300–12324 12462–12440	162	62	45
R. typhi groEL (AF462073)	Forward primer: 5′-GGTAGAAATGTACTTATCGAACAATC-3′ Reverse primer: 5′-GTAGCAGCAAGCGCATCTTCAACGCG-3′	640–665 1720–1745	1,080	55	45

[a] Product of *rrp* forward primer and *invA*R140.

replication and growth within the host cell cytoplasm, and exit (as diagrammed in Fig. 1A). The host cell β-actin was effectively amplified by RT-PCR, reflecting the efficiency of the reactions in which the high-quality templates were added in similar quantities (Fig. 1B). Likewise, when samples were assayed for expression of the rickettsial 16S rRNA gene, amplification was observed for all samples except the uninfected control, confirming that rickettsial RNA was present in sufficient quantity and quality to allow for detection (Fig. 1B). The kinetics of *invA* transcription during in vitro rickettsial infection are shown in Fig. 1B and C. Expression of *invA* was temporarily upregulated during the early stages of infection, attachment, and internalization (time zero to 30 min after induced infection occurred) (Fig. 1B and C). After internalization, *invA* transcriptional levels decreased and remained relatively low during 1 to 8 h postinfection. The *invA* expression level increased during the doubling time of the rickettsiae (12 h postinternalization) and peaked at 24 h postinfection. At 8 days postinfection, we observed that the infected Vero cells began to detach from the surface of the tissue culture flask, indicating host cell destruction by *R. prowazekii*; at that time, *invA* was again upregulated (Fig. 1B and C). At this point, 85% of the cells were heavily infected with *R. prowazekii.*

Although semiquantitative RT-PCR allowed us to monitor expression of *invA* during rickettsial attachment, invasion, and replication in host cells, the assay presents limitations in that it requires post-PCR electrophoresis, gel imaging, and densitometry analysis. Therefore, we were interested in utilizing real time Q-RT-PCR to more easily quantify transcription of *invA* during host cell infection. This technique has been proven to be a very accurate and sensitive tool for reproducible results for gene quantification and requires no post-PCR manipulation. Initially, real-time assays for β-actin, 16S rRNA, and *invA* were done using the DNA-binding dye SYBR Green. Satisfactory results were observed for the majority of the β-actin and for 16S rRNA RT-PCRs. However, C_t values for the *invA* gene were consistently higher than those of the negative (no-template) controls and therefore could not be distinguished from background signals generated by primer dimer artifacts. Consequently, TaqMan probes specific to the genes of interest were used for all subsequent real-time amplification assays.

As evidenced by the consistently intense fluorescence for the β-actin TaqMan probe (Fig. 2C) and the 16S rRNA (Fig. 2B), it was confirmed that the RNAs extracted from infected Vero cells and the resultant cDNAs were of good quality for use in real-time RT-PCR, and the samples contained a sufficient quantity and quality of rickettsial RNA to allow for further detection of specific rickettsial gene expression. The two-step TaqMan probe Q-RT-PCR assays were conducted on the cDNAs generated from samples representing specific stages of the rickettsial life cycle in host cells. The preinfection, 12-h, and 24-h time points were the only ones with consistent *invA* expression for all three replicates, while analysis of *invA* expression within each replicate indicated some variability

TABLE 2. Primers and probes for real time Q-RT-PCR[a]

Gene, primer, and probe	Sequence	GenBank no or nt position
R. prowazekii 16S rRNA		M21789
Forward primer	5′ GTCAGCTCGTGTCGTGAGAT 3′	1032–1051
Reverse primer	5′ TAAGGGCCATGATGACTTGA 3′	1182–1201
Probe	5′(FAM)-TTTGCCAGTGGGTAATGCCG-(TAMRA) 3′	1092–1111
R. prowazekii invA		AJ235271
Forward primer	5′ AGGCGAAACACCAAGTATTG 3′	12719–12738
Reverse primer	5′ TCCACGAAAATTACCGTTCC 3′	12458–12439
Probe	(FAM) 5′ TGCTGGTATAGTTATGATGTACCAAGCTTT-(TAMRA) 3′	12353–12382

[a] Abbreviations: FAM, 6-carboxy fluorescein; TAMRA, rhodamine; nt, nucleotide.

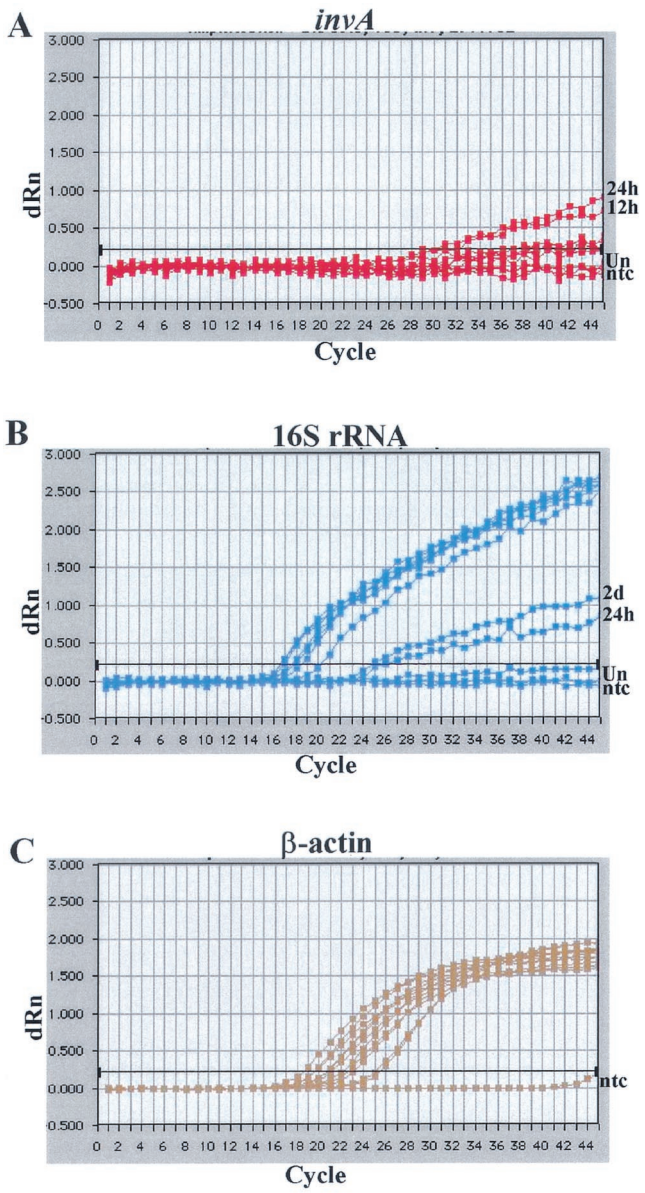

FIG. 2. Kinetics of *invA* transcription during in vitro rickettsial infection as determined by real-time two-step Q-RT-PCR. Transcription of *invA* during various stages of rickettsial intracellular growth was detected with real-time fluorogenic probe-based RT-PCR. Fluorescence emission (corrected for background) is plotted on the *y* axis, and cycle number is on the *x* axis. Amplification plots obtained for *invA* (A), rickettsial 16S rRNA (B), and host cell β-actin (C) are shown.

among time points (Table 3). In addition, the time-dependent profile of *invA* transcription during in vitro rickettsial infection as measured by real-time two-step RT-PCR was similar to that obtained by the conventional RT-PCR. For example, in one replicate where almost all samples were detected, expression of *invA* was detected at the preinfection time point, although at a low level. The transcript slightly increased during internalization (10 to 30 min) and decreased below detectable levels during intracytoplasmic living (1 to 8 h) (Table 3). At doubling time (8 to 12 h), *invA* gene expression resumed and reached a 1,000-fold increase at the 24-h time point (Table 3). The relatively high C_t values displayed by all of the samples during the preinfection to the 12-h time periods made it difficult to identify from the amplification plots any of these samples as being indicative of *invA* expression unique to the internalization process or early intracellular colonization (Fig. 2A). This is in contrast to the results obtained with agarose gel electrophoresis of conventional semiquantitative RT-PCR products, in which the preinfection, 10-min, and 30-min samples had greater PCR products compared to the 1- to 12-h time points (Fig. 1B).

To improve the detection limit of *invA* transcripts, single-tube RT-PCR assays were conducted on the samples collected during the first 24 h postinfection. The rationale for utilizing this technique was based on the concept that RT products generated by gene-specific primers, rather than random hexamers, would contain a higher percentage of rickettsia-specific sequences. Compared to the two-step RT-PCR, we consistently observed increased the number of positives among the various time points; however, C_t values for these samples remained high (Table 4 and Fig. 3). Taken together, the data

TABLE 3. Quantification of *invA* transcript levels during *R. prowazekii* infection in Vero cells by real-time two-step fluorescent probe-based quantitative RT-PCR[a]

Time postinfection	Relative *invA* expression ($\Delta\Delta C_t$)[b] of replicate no.:		
	1	2	3
0 min	1	1	194
10 min	1.3	0	0
30 min	0	5.2	0
1 h	7.4	0	0
2 h	2.8	0	0
4 h	0	5.2	1.0
8 h	5.2	0	0
12 h	90.5	32	512
24 h	2×10^5	5×10^4	3×10^5
2 days	0	0	119.4
8 days	0	64	0

[a] The data are presented as the relative expression of *invA* normalized to that of the endogenous reference, rickettsial 16S rRNA. For each replicate, the sample-time point combination with the lowest level of *invA* gene expression was designated as a calibrator, with a gene expression level set at 1.0.
[b] C_t = 45 cycles (no amplification).

TABLE 4. Quantification of *invA* transcript levels during *R. prowazekii* infection in Vero cells by real-time single-step fluorescent probe-based quantitative RT-PCR[a]

Time postinfection	Relative *invA* expression ($\Delta\Delta C_t$) of replicate no.:		
	1	2	3
0 min	101.1	2.0	36.7
10 min	75.0	9.9	70.5
30 min	62.6	10.4	328.5
1 h	34.3	18.7	9,607.8
4 h	6.8	1.0	34.0
12 h	1.0	2.2	1.0
24 h	9,607.8	568.0	2,797.6

[a] Data are presented as the relative expression of *invA* normalized with the C_t value of the endogenous reference, rickettsial 16S rRNA. For each replicate, the sample-time point combination with the lowest level of *invA* gene expression was designated as a calibrator, with a gene expression level set at 1.0.

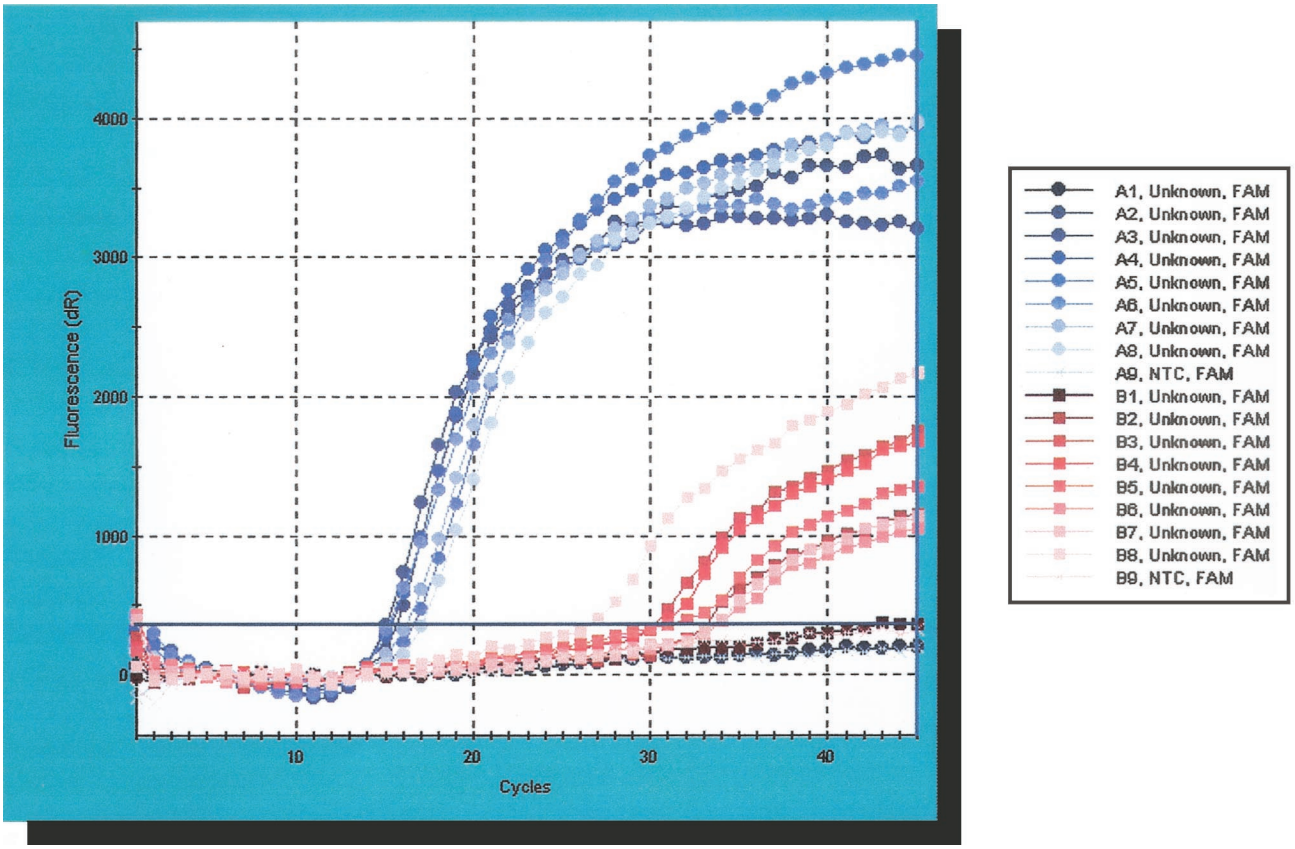

FIG. 3. Amplification plots for *invA* and 16S rRNA transcripts during various stages of rickettsial infection in Vero cells, as determined by real-time single-step Q-RT-PCR. Fluorescence emission (corrected for background) is plotted on the *y* axis and cycle number is on the *x* axis.

indicated that the low levels of *invA* expression were reflective of mRNA production by the rickettisae and not due to poor RT and amplification. As summarized in Table 4, for all three replicates the 12-h sample was designated the calibrator, and the pattern of *invA* expression was similar to conventional RT-PCR results. Increasing from the baseline set at time zero during internalization, *invA* expression decreased and remained low during the period of 1 to 12 h postinfection, prior to increasing at the 24-h time point.

The *invA* mean C_t value for the 24-h time point for the three replicates of single-tube RT-PCR was 28.18 ($\pm$ 2.90); this was smaller than the means observed for all other time points (33.20, 31.55, 31.12, 31.88, 34.53, and 37.44 for the preinfection, 10-min, 30-min, 1-h, 4-h, and 12-h samples, respectively). The low number of samples per group ($n = 3$, $N = 20$; between-group df = 6, within-group df = 14) makes a formal statistical interpretation of the results problematic, but a one-way ANOVA comparison of the mean C_t values for each of the seven time points was not significant ($F = 1.75 < F_{0.05,\ 6,\ 14} = 2.85$; $P = 0.187$). However, two multiple comparison tests (Duncan's New Multiple Range test and Fisher's least significant difference method) showed significant differences between the 12- and 24-h mean C_t values. We interpret these results to indicate that *invA* expression was increased at 24 h postinfection compared to levels at earlier time points.

Was the increase in *invA* expression observed at 24 h postinfection in the three single-tube RT-PCR replicates (i) an artifact due to a concomitant increase in rickettsiae within the host cells, or (ii) a genuine reflection of upregulated mRNA expression? If scenario (i) were true, than we would expect to see a significantly smaller mean C_t value for the 16S rRNA RT-PCR at 24 h postinfection compared to all other time points, indicative of the increased quantity of rickettsia within these host cells. A one-way ANOVA conducted on the 16S rRNA mean C_t values for all seven time points showed no significant differences between them ($F = 2.43 < F_{0.05,\ 6,\ 14} = 2.85$; $P = 0.079$). Duncan's New Multiple Range test indicated significant differences between the 1-h versus 24-h and between the 10-min versus 30-min time points, while Fisher's least significant difference method showed significant differences between the 1- versus 24-h time points and between the 10- and 30-min versus 4-h time points. A third multiple comparisons test, the Student-Newman-Keuls method, showed no differences between any time points.

As with the *invA* ANOVA results, the small number of per-group replicates ($n = 3$) means these statistics should be interpreted with some caution; however, we concluded that they indicate that the increase in *invA* expression is not an artifact of rickettsial replication in the host cells.

To investigate if *invA* expression is correlated to stress conditions resulting from invasion and intracellular survival, the expression of rickettsial *groEL* was assessed as a molecular determinant of stress conditions. Analysis of the RT-PCR in-

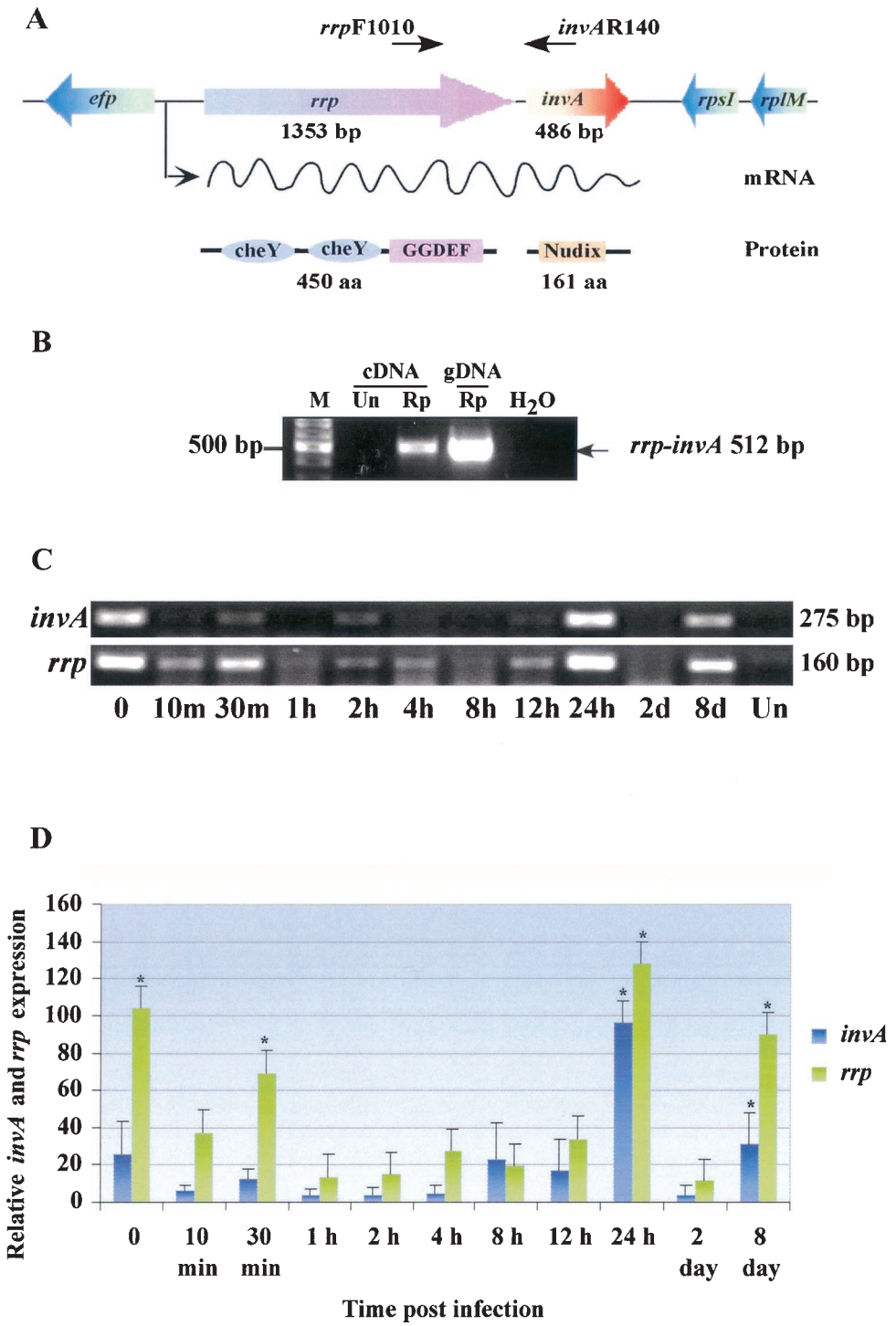

FIG. 4. Structure and RT-PCR analysis of the *rrp-invA* operon-like gene cluster in *R. prowazekii*. (A) Schematic structure of the *rrp-invA* operon-like gene cluster in *R. prowazekii* illustrates the two open reading frames of the 1,353-bp *rrp* and the 486-bp *invA,* separated by 29 nucleotides, located between the gene encoding elongation factor P (*efp*) and the ribosome S9 gene (*rpsI*). *rrp* encodes a response regulator homolog protein in which GGDEF and two cheY homolog domains are found in series from the N to C terminal. *invA* encodes an invasion protein A with a Nudix motif at the N terminus. (B) Analysis of *rrp-invA* operon-like gene cluster by RT-PCR. DNase-treated total RNA was reverse transcribed to generate cDNA before it was subjected to PCR utilizing forward (*rrp*F1010) and reverse (*invA*R140) primers. Products were electrophoresed on a 1% agarose gel stained with ethidium bromide. Un, uninfected Vero cells; Rp, *R. prowazekii*-infected cells; H_2O, reagent control. Lane M, DNA size markers, as indicated on the left. (C) The transcriptional profiles of *rrp* and *invA* during rickettsial intracellular growth cycle were determined by semiquantitative RT-PCR. Amplified products were electrophoresed on 1% agarose gels stained with ethidium bromide, shown in negative. The sizes of amplified fragments are indicated on the right. (D) Densitometric analysis of *invA* and *rrp* expression levels. The levels of expression were quantitated by using the densitometry function of the Alpha Imager software. The densitometric result of each time point was normalized to the internal control running in parallel. The ratio of sample intensity to that of the corresponding internal control, expressed as the mean ± standard error, was plotted on the *y* axis against time postinfection. A one-way ANOVA was used to determine statistical differences between columns (treatment) and within columns (residual). ∗, significant difference at a P level of <0.05.

dicates that expression of rickettsial *groEL* and *invA* had similar profiles early after infection (Fig. 1B).

Because *invA* is located downstream from a gene encoding a response regulator protein homolog (*rrp*) (Fig. 4A), a part of a two-component signal transduction system, we examined the transcription of *invA* in relation to the *rrp* of the signal transduction system. RT-PCR utilizing a forward primer from *rrp* and reverse primer from *invA* was performed on cDNA of *R. prowazekii*-infected Vero cells which was previously verified to be without DNA contamination. The expected fragment of 512 bp was amplified from *R. prowazekii*-infected Vero cell cDNA and the genomic DNA of *R. prowazekii* (Fig. 4B). The intact mRNA spanning the 3′ end of *rrp* and 5′ region of *invA* was detected, indicating the polycistronic transcription of the two genes, *rrp* and *invA*, and their arrangement as an operon. The transcription profile of *rrp* during the rickettsial intracellular growth cycle was determined by semiquantitative RT-PCR to be differentially expressed during rickettsial infection (Fig. 4C and D). Furthermore, the pattern of *rrp* expression was similar to that observed for rickettsial *invA*.

DISCUSSION

The members of typhus group rickettsiae enter, replicate in the cytoplasm, and exit upon host cell lysis (12). Thus, rickettsial pathogenesis is attributed to their ability to infect and lyse host cells. However, the molecular mechanisms of rickettsial pathogenesis are not well defined. We have been systematically examining a number of putative rickettsial virulence genes to improve our understanding of this process. Among these, an invasion gene homolog, *invA* of *R. prowazekii*, has recently been characterized as encoding a Nudix hydrolase subfamily, dinucleoside oligophosphate pyrophosphatase, which preferentially degrades a group of minor nucleosides implicated in cellular stress response signaling (10). Based on the enzymatic activity of *R. prowazekii* InvA, we postulated that this protein might facilitate rickettsial intracellular survival during the oxidative stress following host cell invasion (10). In this study, we further characterized *R. prowazekii invA* transcriptional profiles during the rickettsial growth cycle in Vero cells. Using RT-PCR and real-time fluorescent probe-based Q-RT-PCR, differential expression of rickettsial *invA* was observed during the various time points postinfection. We report that *invA* expression was upregulated at early infection (within 30 min after internalization), 24 h postinfection, and at late infection at day 8 postinfection. All the time points selected represent specific stages in which rickettsiae experience stress, including entry, escape from the phagosome, growth within the host cell cytoplasm, and exit. Although not addressed in the present study, we speculate that the presence of *invA* transcripts as early as the initial rickettsial attachment to the host cell may correlate with the biological finding that only metabolically active rickettsiae can induce host cell phagocytosis and gain access to nonphagocytic epithelial and endothelial cells (12).

A number of studies of facultative intracellular pathogens have suggested that *groEL* is upregulated under a range of environmental stress conditions following host cell entry (1, 8, 9, 16, 22). Therefore, we have used rickettsial *groEL* expression as a marker of stress condition. Our experiment showed that the expression pattern of *groEL* at an early stage of infection was similar to that described for *invA*. These results support our hypothesis and previous finding that rickettsial InvA functions in response to stress during rickettsial internalization to facilitate bacterial survival during entry (10). In both cases, successful entry of rickettsiae into the host cell, generation of progeny, and exit are examples of their adaptation to stressful conditions. Under such stress conditions, Nudix hydrolase transcription and expression may function as a buffer, enhancing rickettsial survival within the cytoplasm of eukaryotic cells. The ability of intracellular pathogens to sense and adapt to the hostile environment of the host cell is an important factor governing virulence.

Although we knew very little about rickettsial gene regulation, the analysis of recently published genome data revealed that the 486-bp *invA* is located downstream of *rrp*, a 1.3-kb gene encoding a response regulator protein homolog of two-component signal transduction systems (3, 18). Rrp, a 450-residue protein, belongs to the PleD-like response regulator family, with the C-terminal phosphoesterase-GGDEF domain and two cheY-homologous receiver domains located at the N terminus (Domain Architecture Retrieval Tool [http://www.ncbi.nlm.nih.gov] and references 2 and 13). A well-defined response regulator protein in this family, PhoP of *Yersinia pestis*, has been demonstrated to be important for virulence and survival under conditions of macrophage-induced stress (19). As shown in Fig. 4A, *rrp* and *invA* open reading frames are oriented in the same direction and are separated by an intergenic region of 29 nucleotides. Based on computer analysis, it is likely that these two genes are arranged into an operon, because the putative promoter sequences are only found upstream of the *rrp* gene. Here, we have shown evidence that *rrp* and *invA* are organized in an operon and that they are cotranscribed. Despite the suggested regulatory function based on the high homology to several response regulator proteins, we have no experimental evidence to support the notion that the rickettsial Rrp may also function as a response regulator protein. The expression of dinucleoside oligophosphate pyrophosphatase may be regulated by the part of the two-component signal transduction system that is similar to what has been described for response regulators in other bacterial systems.

ACKNOWLEDGMENTS

This work was supported in part by National Institutes of Health grant AI 17828. J.G. received a predoctoral fellowship support from the Royal Thai Army, Ministry of Defense, Thailand.

REFERENCES

1. **Abu Kwaik, Y., B. L. Eisenstein, and N. C. Engleberg.** 1993. Phenotypic modulation by *Legionella pneumophila* upon infection of macrophages. Infect. Immun. **61:**1320–1329.
2. **Aldridge, P., and U. Jenal.** 1999. Cell cycle-dependent degradation of a flagellar motor component requires a novel-type response regulator. Mol. Microbiol. **32:**379–391.
3. **Andersson, S. G. E., A. Zomorodipour, J. O. Andersson, T. Sicheritz-Ponten, U. C. M. Alsmark, R. M. Podowski, A. K. Naslund, A. S. Eriksson, H. H. Winkler, and C. G. Kurland.** 1998. The genome sequence of *Rickettsia prowazekii* and the origin of mitochondria. Nature **396:**133–140.
4. **Azad, A. F., and C. B. Beard.** 1998. Rickettsial pathogens and their arthropod vectors. Emerg. Infect. Dis. **4:**179–186.
5. **Azad, A. F.** 1988. Relationship to vector biology and epidemiology of louse and flea-borne rickettsioses, p. 52–62. *In* D. H. Walker (ed.), Biology of rickettsial diseases. CRC Press, Boca Raton, Fla.
6. **Badger, J. L., C. A. Wass, and K. S. Kim.** 2000. Identification of *Escherichia coli* K1 genes contributing to human brain microvascular endothelial cell invasion by differential fluorescence induction. Mol. Microbiol. **36:**174–182.

7. **Badger, J. L., and K. S. Kim.** 1998. Environmental growth conditions influence the ability of *Escherichia coli* K1 to invade brain microvascular endothelial cells and confer serum resistance. Infect. Immun. **66:**5692–5697.
8. **Buchmeier, N. A., and F. Heffron.** 1990. Induction of *Salmonella* stress protein upon infection of macrophages. Science **248:**730–732.
9. **Gahan, C. G. M., J. O'Mahony, and C. Hill.** 2001. Characterization of the *groESL* operon in *Listeria monocytogenes*: utilization of two reporter systems (*gfp* and *hly*) for evaluating in vivo expression. Infect. Immun. **69:**3924–3932.
10. **Gaywee, J., W.-L. Xu, S. Radulovic, M. J. Bessman, and A. F. Azad.** 2002. The *Rickettsia prowazekii* invasion gene homolog (*invA*) encodes a Nudix hydrolase active on adenosine (5′)-pentaphospho-(5′)-adenosine. Mol. Cell. Proteomics **1:**179–185.
11. **Gibson, U. E. M., C. A. Heid, and P. M. Williams.** 1996. A novel method of real time quantitative RT-PCR. Genome Res. **6:**995–1001.
12. **Hackstadt, T.** 1996. The biology of rickettsiae. Infect. Agents Dis. **5:**127–143.
13. **Hecht, G. B., and A. Newton.** 1995. Identification of a novel response regulator required for the swarmer-to-stalked-cell transition in *Caulobacter crescentus.* J. Bacteriol. **177:**6223–6229.
14. **Higgins, J. A., S. Radulovic, B. H. Noden, J. M. Troyer, and A. F. Azad.** 1998. Reverse transcriptase PCR amplification of *Rickettsia typhi* from infected mammalian cells and insect vectors. J. Clin. Microbiol. **36:**1793–1794.
15. **Lau, A. O. T., J. B. Sacci, Jr., and A. F. Azad.** 2001. Host responses to *Plasmodium yoelii* hepatic stages: a paradigm in host-parasite interaction. J. Immunol. **166:**1945–1950.
16. **Lin, J., and T. A. Ficht.** 1995. Protein synthesis in *Brucella abortus* induced during macrophage infection. Infect. Immun. **63:**1409–1414.
17. **Mitchell, S. J., and M. F. Minnick.** 1995. Characterization of a two-gene locus from *Bartonella bacilliformis* associated with the ability to invade human erythrocytes. Infect. Immun. **63:**1552–1562.
18. **Ogata, H., S. Audic, P. Renesto-Audiffren, P. E. Fournier, V. Barbe, D. Samson, V. Roux, J. Weissenbach, J. M. Claverie, and D. Raoult.** 2001. Selfish DNA in protein-coding genes of *Rickettsia*. Science **293:**2093–2098.
19. **Oyston, P. C., N. Dorrell, K. Williams, S. R. Li, M. Green, R. W. Titball, and B. W. Wren.** 2000. The response regulator PhoP is important for survival under conditions of macrophage-induced stress and virulence in *Yersinia pestis*. Infect. Immun. **68:**3419–3425.
20. **Radulovic, S., H. M. Feng, M. Morovic, B. Djelalija, V. Popov, P. Crocquet-Valdes, and D. H. Walker.** 1996. Isolation of *Rickettsia akari* from a patient in a region where Mediterranean spotted fever is endemic. Clin. Infect. Dis. **22:**216–220.
21. **Raoult, D., J. B. Ndihokubwayo, H. Tissot-Dupont, V. Roux, B. Faugere, R. Abegbinni, and R. J. Birtles.** 1998. Outbreak of epidemic typhus associated with trench fever in Burundi. Lancet **352:**353–358.
22. **Yamamoto, T., T. Hanawa, and S. Ogata.** 1994. Induction of *Yersinia enterocolitica* stress proteins by phagocytosis with macrophage. Microbiol. Immunol. **38:**295–300.

Editor: J. T. Barbieri